SPANDIDOS PUBLICATIONS

INTERNATIONAL JOURNAL OF ONCOLOGY 56: 581-595, 2020

The GALNT6-LGALS3BP axis promotes breast cancer cell growth

RYUICHIRO KIMURA[1,8*], TETSURO YOSHIMARU[1,2*], YOSUKE MATSUSHITA[1,2*], TAISUKE MATSUO[1], MASAYA ONO[3], JAE-HYUN PARK[4], MITSUNORI SASA[5], YASUO MIYOSHI[6], YUSUKE NAKAMURA[7] and TOYOMASA KATAGIRI[1,2]

[1]Division of Genome Medicine, Institute of Advanced Medical Sciences; [2]Research Cluster on Integrated Cancer Drug Discovery, Tokushima University, Tokushima, Tokushima 770-8503; [3]Division of Chemotherapy and Clinical Research, National Cancer Center Research Institute, Tokyo 104-0045; [4]Cancer Precision Medicine, Inc., Kawasaki, Kanagawa 210-0821; [5]Department of Surgery, Tokushima Breast Care Clinic, Tokushima, Tokushima 770-0052; [6]Department of Surgery, Division of Breast and Endocrine Surgery, Hyogo College of Medicine, Nishinomiya, Hyogo 663-8501; [7]Cancer Precision Medicine Center, Japanese Foundation for Cancer Research, Tokyo 135-8550, Japan

Received May 20, 2019; Accepted October 24, 2019

DOI: 10.3892/ijo.2019.4941

Abstract. Polypeptide N-acetylgalactosaminyltransferase 6 (GALNT6), which is involved in the initiation of *O*-glycosylation, has been reported to play crucial roles in mammary carcinogenesis through binding to several substrates; however, its biological roles in mediating growth-promoting effects remain unknown. The present study demonstrated a crucial pathophysiological role of GALNT6 through its *O*-glycosylation of lectin galactoside-binding soluble 3 binding protein (LGALS3BP), a secreted growth-promoting glycoprotein, in breast cancer growth. The Cancer Genome Atlas data analysis revealed that high expression levels of GALNT6 were significantly associated with poor prognosis of breast cancer. GALNT6 *O*-glycosylated LGALS3BP in breast cancer cells, whereas knockdown of GALNT6 by siRNA led to the inhibition of both the *O*-glycosylation and secretion of LGALS3BP, resulting in the suppression of breast cancer cell growth. Notably, LGALS3BP is potentially *O*-glycosylated at three sites (T556, T571 and S582) by GALNT6, thereby promoting autocrine cell growth, whereas the expression of LGALS3BP with three Ala substitutions (T556A, T571A and S582A) in cells drastically reduced GALNT6-dependent LGALS3BP *O*-glycosylation and secretion, resulting in suppression of autocrine growth-promoting effect. The findings of the present study suggest that the GALNT6-LGALS3BP axis is crucial for breast cancer cell proliferation and may be a therapeutic target and biomarker for mammary tumors.

Correspondence to: Professor Toyomasa Katagiri, Division of Genome Medicine, Institute of Advanced Medical Sciences, Tokushima University, 3-18-15 Kuramoto-cho, Tokushima, Tokushima 770-8503, Japan
E-mail: tkatagi@genome.tokushima-u.ac.jp

Present address: [8]Department of Pathology, Faculty of Medicine, Kindai University, 377-2 On-higashi, Osaka-sayama, Osaka 589-8511, Japan

[*]Contributed equally

Key words: polypeptide N-acetylgalactosaminyltransferase 6, lectin galactoside-binding soluble 3 binding protein, *O*-glycosylation, secretion, autocrine

Introduction

Mucin-type *O*-glycosylation is a fundamental post-translational modification in secreted or membrane-associated proteins. The first step in *O*-glycan biosynthesis is catalyzed by a large family of polypeptide N-acetylgalactosaminyltransferases (GALNTs) that transfer N-acetylgalactosamine (GalNAc) to serine or threonine residues on the target proteins (1-4). Aberrant *O*-glycosylation of cancer cells affects their growth and survival and their ability to invade and metastasize (5). Accumulating evidence has demonstrated that dysregulation of GALNT expression results in aberrant *O*-glycosylation in breast cancer cells (6). Among the GALNTs, GALNT6 is upregulated in breast (7-11), ovarian (12,13), renal cell (14), lung (15) and pancreatic (16) cancers. Notably, an increasing number of studies have demonstrated that GALNT6 controls cancer cell proliferation, migration and invasion abilities through the regulation of mucin (MUC)1 (10), fibronectin (17), MUC4 (18), glucose-regulated protein 78 (GRP78) (19), estrogen receptor (ER) (20), and epidermal growth factor receptor signaling molecules (12) as its substrates. However, the mechanism through which GALNT6 promotes carcinogenesis is incompletely understood, since its *O*-glycan substrates have not been fully elucidated.

The extracellular matrix protein lectin galactoside-binding soluble 3 binding protein (LGALS3BP) is initially purified and cloned as a ligand of the lactose-specific S-type lectin galectin-3 (formerly Mac-2), which was identified as a heavy glycosylated molecule in the tumor tissues and serum of patients with lung, breast and ovarian cancer (21). LGALS3BP was also identified as a tumor-associated antigen (90K) that

is secreted in the serum in various types of cancer (22-24). Accumulating studies have revealed that elevated serum and tissue levels of LGALS3BP are associated with poor prognosis in several human cancers, including breast cancer, lymphoma, pleural mesothelioma and non-small-cell lung cancer (25-32). However, the molecular mechanism underlying glycosylated LGALS3BP secretion in the serum and tissue of cancer patients has not yet been fully elucidated.

The aim of the present study was to investigate whether GALNT6 directly binds and *O*-glycosylates LGALS3BP, thereby enhancing the secretion of LGALS3BP in breast cancer cells, hoping that the findings may lead to the development of GALNT6-based therapies and novel biomarkers for mammary tumors.

Materials and methods

Cell lines and culture conditions. Human breast cancer cell lines (ZR-75-1, BT-474, SK-BR-3, HCC1569, HCC1954, MDA-MB-231, MDA-MB-468, BT-20, HCC38, HCC70, HCC1395, HCC1806 and HCC1937), a mammary epithelial cell line (MCF-10A) and HeLa cells were obtained from the American Type Culture Collection. MCF-7 cells were obtained from the Health Science Research Resources Bank. 293T cells and MDA-MB-453 cells were provided by the RIKEN BioResource Research Center. All cell lines were cultured under the corresponding depositors' recommendations. The cell line stocks used in the present study had been properly stored in liquid nitrogen. The morphology of these cell lines was monitored by microscopy and confirmed that it was maintained by comparing our images with the original morphological images. No *Mycoplasma* contamination was detected in any of the cultures using a Mycoplasma Detection kit (Takara Bio) and MycoAlert™ Mycoplasma Detection Kit (Lonza).

Plasmids. The pCAGGSnHC vectors expressing wild-type (WT) and inactivated mutant (H271D) GALNT6 in frame with an HA-tag at the carboxyl terminus (GALNT6 WT-HA and GALNT6 H271D-HA) were described previously (10). To construct the LGALS3BP expression vector, the entire coding sequence of LGALS3BP complementary DNA was amplified by reverse transcription (RT)-polymerase chain reaction (PCR) analysis using KOD -Plus- DNA polymerase (Toyobo Life Science) and cloned into the pCAGGSn3FC expression vector in frame with a FLAG-tag at the carboxyl terminus (LGALS3BP-FLAG). The following primer set was used for LGALS3BP-WT amplification: 5'-ATAAGAATGCGGCCGCATGACCCCTCCGAGGCTC-3' (forward) and 5'-CCGCTCGAGGTCCACACCTGAGGAGTTG-3' (reverse). The underlined sequences indicate the *Not*I and *Xho*I sites, respectively. In addition to full-length LGALS3BP (1-585), expression plasmids for the LGALS3BP deletion mutants Del-1 (1-538) and Del-2 (1-560) were prepared by PCR. The amplification conditions were as follows: 94˚C for 2 min, followed by 30 cycles of denaturing, annealing and extension (94˚C for 15 sec, 55˚C for 30 sec and 68˚C for 2 min, respectively). The reverse primers 5'-CCGCTCGAGCTCGAAATCGGTGACGTCTGCCA-3' (Del-1) and 5'-CCGCTCGAGGGGGAAGGAGGAGGTGCTCTTCG-3' (Del-2) were used with the forward primer 5'-ATAAGAATGCGGCCGCATGACCCCTCCGAGGCTC-3'. The LGALS3BP alanine substitution mutants Mut-1 (S546A), Mut-2 (T550A/N551A), Mut-3 (S552A/S553A), Mut-4 (S555A/T556A), Mut-5 (S557A/S558A), Mut-6 (S555A) and Mut-7 (T556A), which were point mutants of LGALS3BP-Del-2 (1-560)-FLAG, and the T556A, T571A, T556A/T571A, T579A, N580A, S581A, S582A and T556A/T571A/S582A mutants of full-length *LGALS3BP*-FLAG, were generated by conventional two-step mutagenesis PCR.

LGALS3BP-FLAG- and GALNT6-FLAG-expressing pQCXIP (Takara Bio) retroviral vectors were generated using PCR primers. The following primer set was used to amplify LGALS3BP-FLAG: 5'-ATAAGAATGCGGCCGCATGACCCCTCCGAGGCTC-3' (forward) and 5'-CCGGATCCTTACTTGTCGTCATCGTCTTTGTAGTCGTCCACACCTGAGGAGTTG-3' (reverse). The underlined sequences indicate the *Not*I and *Bam*HI sites, respectively; the double underlining indicates the FLAG-tag sequence. The following primer set was used to amplify GALNT6-FLAG: 5'-GGGGCGGCCGCCACCATGAGGCTCCTCCGCAGACGCCA-3' (forward) and 5'-CCGAATTCTCACTACTTGTCGTCATCGTCTTTGTAGTCGACAAGAGCCACAACTGATGGG-3' (reverse). The underlined sequences indicate the *Not*I and *Bam*HI sites, respectively; the double underlining indicates the FLAG-tag sequence.

Transfection and viral infection. 293T and HeLa cells were transfected with expression vectors using FuGENE 6 (Promega Corporation). Plat-E cells were kindly provided by Dr Toshio Kitamura (University of Tokyo) and were co-transfected with retroviral vectors and pVSV-G using FuGENE HD (Promega Corporation), according to the manufacturer's instructions. Culture supernatants were collected 48 h after transfection. ZR-75-1 and HCC1806 cells were infected with the culture supernatants in the presence of polybrene. Infected cells were then selected in the presence of puromycin.

For gene silencing via RNA interference, ZR-75-1 and BT-20 cells were transfected with siRNA oligonucleotides (Sigma-Aldrich Japan KK) using Lipofectamine RNAiMAX (Thermo Fisher Scientific, Inc.). The sequences targeting enhanced green fluorescent protein (*EGFP*), *GALNT6* #1, *LGALS3BP* #1 or *LGALS3BP* #2 were as follows: 5'-GCAGCACGACUUCUUCAAG-3' for *EGFP*, 5'-GAGAAAUCCUUCGGUGACA-3' for *GALNT6* #1, 5'-GCGUGAACGAUGGUGACAU-3' for *LGALS3BP* #1, and 5'-UCACCCUGUCGUCAGUCAA-3' for *LGALS3BP* #2.

Immunoprecipitation (IP). Cells were lysed with lysis buffer [50 mM Tris-HCl (pH 7.5), 150 mM NaCl, 5 mM 2-mercaptoethanol, 0.1% NP-40 and 0.5% CHAPS]. Cell supernatants and cell lysates were immunoprecipitated with anti-FLAG M2 affinity gel (Sigma-Aldrich; Merck KGaA). Immunoprecipitated protein complexes were washed three times with lysis buffer. Immunoprecipitates were separated using 10% SDS-PAGE and analyzed by immunoblotting.

Immunoblotting analysis and silver staining. The protein solutions were mixed with SDS-lysis buffer [125 mM Tris-HCl (pH 6.8), 4% SDS, 20% glycerol, 0.04% bromophenol blue and 10% 2-mercaptoethanol] to prepare the samples for

SDS-PAGE analysis. To denature the proteins, the mixed solution was heated at 95˚C for 5 min. Equal volumes of cell lysate (5 μl; 1% of whole-cell lysates, 10% of immunoprecipitates) were loaded and resolved on 10% SDS-PAGE gels. Lysates were electrophoretically separated, blotted onto nitrocellulose membranes, and blocked with 4% Block Ace solution (Dainippon Pharmaceutical) for 3 h at room temperature. The membranes were subsequently incubated for 12 h at 4˚C with antibodies against the following proteins: FLAG-tag (M2, mouse monoclonal, 1:5,000, cat. no. F3165, Sigma-Aldrich; Merck KGaA), HA tag (3F10; rat monoclonal, 1:3,000, cat. no. 11867423001, Roche Diagnostics GmbH), LGALS3BP (rabbit polyclonal, 1:1,000, cat. no. NBP1-89346, Novus Biologicals), GALNT6 (rabbit polyclonal, 1:500) (10) and actin (AC-15, mouse monoclonal, 1: 5,000, cat. no. A1978, Sigma-Aldrich; Merck KGaA). Following incubation with a horseradish peroxidase (HRP)-conjugated secondary antibody (anti-mouse IgG-HRP, polyclonal, 1:5,000, sc-2005; anti-rat IgG-HRP, polyclonal, 1:5,000, sc-2006; anti-rabbit IgG-HRP, polyclonal, 1:1,000, sc-2004; Santa Cruz Biotechnology, Inc.), the blots were developed using an enhanced chemiluminescence system (GE Healthcare) and scanned using an Image Reader LAS-3000 mini (Fujifilm). *Vicia villosa* agglutinin (VVA) lectin blot analysis was performed using biotin-conjugated VVA lectin (cat. no. BA-3601-1, EY Laboratories) and streptavidin-HRP (cat. no. 554066, BD Biosciences), as described previously (10). Silver staining for 30 sec at room temperature was performed using a Silver Stain MS Kit (Wako Pure Chemical Industries, Ltd.). Full-length images of the immunoblots are shown in the Supplementary Figures.

2-Dimensional image-converted analysis of liquid chromatography-mass spectrometry (LC-MS) (2DICAL). Cell lines stably expressing GALNT6-HA or mock vector were established as described previously (10). Cells were lysed in 0.5% NP-40 immunoprecipitation lysis buffer at 4˚C for 30 min and were then incubated with anti-HA agarose beads (Sigma-Aldrich; Merck KGaA) at 4˚C for 16 h. After washing with the same buffer, the proteins bound to the beads were eluted with 1% sodium deoxycholate buffer. Subsequently, samples were prepared for LC-MS as described previously (33).

Immunocytochemistry. Cells were fixed with 4% paraformaldehyde for 30 min at 4˚C and incubated with mouse anti-FLAG-tag M2 (Sigma-Aldrich; Merck KGaA), rat anti-HA-tag (Roche Diagnostics GmbH), rabbit anti-FLAG-tag (Sigma-Aldrich; Merck KGaA), mouse anti-Golgi-58k (Sigma-Aldrich; Merck KGaA), and rabbit anti-GALNT6 (10) antibodies. The nuclei were counterstained with 4',6-diamidino-2-phenylindole (DAPI). Fluorescent images were obtained with Olympus IX71 and FV3000 microscopes (Olympus Corporation).

Reverse transcription-quantitative PCR (RT-qPCR) analysis. Expression of the *GALNT6* and *LGALS3BP* genes was evaluated by RT-qPCR. Total RNA was extracted, and complementary DNA was subsequently synthesized. The complementary DNA was analyzed by qPCR using a 7500 Real-Time PCR system (Thermo Fisher Scientific, Inc.) and SYBR Premix ExTaq (Takara Bio) according to the manufacturer's instructions. The thermocycling conditions were as follows: 10 min at 94˚C, followed by 40 cycles of denaturation at 94˚C for 15 sec, 1 min annealing and extension at 60˚C, and reading of the fluorescence. Following threshold-dependent cycling, melting curve analysis was performed from 60 to 94˚C. Gene expression in each sample was normalized to the β2-MG mRNA content and quantified using the $2^{-\Delta\Delta Ct}$ method. The following primers were used: *GALNT6*, 5'-GCAGAGGTC TGGATGGACAGCTA-3' and 5'-GGTAGACATTGTGCA GGTACCAG-3'; *LGALS3BP*, 5'-GCCCCTTCTACCTGA CCAA-3' and 5'-TGAGTAGGGCGACATCTGG-3'; *GALNT3*, 5'-ATGCCTTGCTCTGTTGTTGG-3' and 5'-TGGTTTGCC TCCTTGATTGT-3'; and *β2-MG*, 5'-AACTTAGAGGTGGGG AGCAG-3' and 5'-CACAACCATGCCTTACTTTATC-3'.

Determination of LGALS3BP in the culture supernatant by immunoblotting analysis. The extracellular release of LGALS3BP from the cells were evaluated by immunoblotting. Briefly, ZR-75-1, BT-20 and SK-BR-3 cells were transfected with siRNA against GALNT6 or LGALS3BP, and the culture medium was changed to 0.1% FBS in medium at 48 h post-transfection. After 24 h, the culture medium was collected and filtered, followed by acetone precipitation at -30˚C for 2 h, and subsequently centrifuged at 22,000 x g for 30 min. The pellets were dried and lysed with SDS-lysis buffer [125 mM Tris-HCl (pH 6.8), 4% SDS, 20% glycerol, 0.04% bromophenol blue and 10% 2-mercaptoethanol]. LGALS3BP in the culture medium was determined using immunoblotting.

Effect of soluble LGALS3BP on the proliferation of HCC1806 cells. HeLa and 293T cells were transfected with GALNT6-HA construct (WT and H271D mutant) and LGALS3BP-FLAG construct. After 24 h, the culture medium was changed to 1% FBS or 2% FBS in medium of HeLa and 293T cells, respectively, and cultured for 72 h. The culture medium was collected and filtered (pore size, 0.22 μm), followed by replacement of each culture medium with the medium of HCC1806 cells. After further culture for 72 and 96 h, cell proliferation was assessed as described below.

LGALS3BP ELISA. The LGALS3BP protein levels in the culture supernatants were quantified using a human galectin-3BP/MAC-2BP Quantikine ELISA Kit (R&D Systems, Inc.) according to the manufacturer's instructions.

Cell proliferation assay. WST-8 assays were performed using a Cell Counting Kit-8 (Dojindo Molecular Technologies, Inc.). A 1:10 dilution of Cell Counting Kit-8 solution was added to the cells and incubated for 1 h. Subsequently, the absorbance at 450 nm was measured to calculate the number of viable cells per well.

In vitro glycosylation assay. In vitro GALNT6 activity toward LGALS3BP as a substrate was assessed as follows (34): Various concentrations of recombinant GALNT6 protein (codons 35-622) were incubated with 2 μM biotin-tagged LGALS3BP peptide (568-585, WT, T571A, S582A and T571A/T582A) and UDP-GalNAc for 3 h at room temperature. The reactions were terminated by the addition of 0.5 M EDTA. These reaction mixtures were then transferred into NeutrAvidin-coated plates (Thermo Fisher Scientific, Inc.) and

incubated for 1 h at room temperature. After the samples were washed with PBS, the α-GalNAc-specific lectin *Helix pomatia agglutinin* conjugated to HRP (HPA-HRP, EY Laboratories) was added and subsequently incubated for 30 min at room temperature. After washing, bound HPA-HRP was quantified by incubation with 3,3',5,5'-tetramethylbenzidine peroxide solution (Thermo Fisher Scientific, Inc.) for 30 min in the dark at room temperature. After HRP activity was terminated with sulfuric acid, the absorbance at 415 nm was measured using a microplate reader (Infinite M200, Tecan).

Proteasome-dependent degradation of LGALS3BP. ZR-75-1 cells were transfected with EGFP or GALNT6 #1 siRNA. After 48 h of transfection, cells were treated with 10 μM MG132 (EMD/Merck KGaA), and harvested at 6 and 12 h after treatment. Immunoblotting analyses were performed using the indicated antibodies.

Analysis of public database. The data for GALNT6 and LGALS3BP mRNA expression (RNA Seq V2 RSEM) in primary invasive breast carcinoma samples were downloaded from The Cancer Genome Atlas (TCGA) network (http://cancergenome.nih.gov/). Kaplan-Meier plots for breast cancer patients were analyzed by the Kaplan-Meier plotter (KM plotter) database (http://kmplot.com/analysis/). Breast cancer patients in the KM plotter database were stratified into 'low' and 'high' GALNT6 mRNA expression groups (Affymetrix ID: 219956_at) based on an autoselected best cutoff value.

Statistical analysis. Data are expressed as the means ± standard deviation (SD). The Student's t-test was used for comparisons between two groups, and one-way analysis of variance with Tukey or Dunnett's post hoc test was applied for multiple comparison. P-values <0.05 were considered to indicate a statistically significant difference. The statistical significance of TCGA datasets was calculated using the Kruskal-Wallis test and Dunnett's post-hoc test with SPSS version 20.0 (IBM Corp.). *GALNT6* and *LGALS3BP* expression in ER-positive or human epidermal growth factor receptor 2 (HER2)-positive samples and a corresponding normal sample were compared using two-tailed Student's t-test.

Results

GALNT6 expression is correlated with breast cancer prognosis. GALNT6 expression has been reported to be upregulated in breast cancer cells (7-10). The association between the *GALNT6* expression level and prognosis for each breast cancer subtype was further investigated via analysis of TCGA public datasets. *GALNT6* expression was found to be higher in patients with ER-positive and HER2-positive invasive breast cancer compared with that in patients with ER-negative or triple-negative breast cancer (Fig. S1A). Moreover, it was confirmed that *GALNT6* was expressed at high levels in breast cancer compared with corresponding normal breast control samples (n=110; Fig. S1B), as reported previously (7,9,10). Of note, *GALNT6* was significantly upregulated in ER- (n=34) and HER2-positive (n=9) breast cancer compared with the corresponding normal controls (Fig. S1C). More importantly, KM plotter database analysis revealed that high expression levels of GALNT6 were correlated with shorter duration of relapse-free survival (P=0.006), distant metastasis-free survival (P=0.00084) and overall survival (P=0.0036) across all breast tumor types (Fig. S1D). Notably, high *GALNT6* expression was positively correlated with reduced relapse-free survival duration compared with that of patients with low *GALNT6* expression in patients with the ER-positive (P=0.0038) and HER2-positive (P=0.032) subtypes of breast cancer (Fig. S1E). In addition, in the ER-negative subtype, high *GALNT6* expression was also associated with reduced relapse-free survival duration (P=0.017; Fig. S1E). These findings strongly support the results of previous studies (7-10) reporting that *GALNT6* plays a crucial role in mammary carcinogenesis and progression of breast cancer, regardless of the ER or HER2 expression status, although *GALNT6* expression was found to be higher in patients with ER-positive and HER2-positive status among all breast tumor types.

Identification of LGALS3BP as a substrate of GALNT6. To further investigate unknown effects of GALNT6 on mammary carcinogenesis and progression of breast cancer, GALNT6-binding protein(s) as substrate(s) were investigated by 2DICAL analysis (35) using a previously established stable cell line (HeLa-GALNT6-WT) (10,17) (Fig. S2A and B). LGALS3BP (also referred to as Mac-2-binding protein or tumor-associated antigen 90K) was identified as a candidate GALNT6-binding protein, as four different peptides derived from the LGALS3BP protein were detected along with three peptides from the GALNT6 protein (Table I). Moreover, LGAL3BP has been identified as a heavy glycosylated molecule in tumor tissues and serum from patients with lung, breast and ovarian cancers (21). Therefore, we focused on LGALS3BP as a strong candidate GLANT6-binding protein.

The expression levels of *GALNT6* and *LGALS3BP* were initially examined in 15 breast cancer cell lines and the normal epithelial cell line MCF 10A by qPCR analysis, and high expression levels of both genes were found in the ZR-75-1, BT-20 and SK-BR-3 cell lines (Fig. S2C). To validate the 2DICAL results, LGALS3BP-FLAG was transfected into ZR-75-1 cells, and cell lysates were immunoprecipitated with an anti-FLAG antibody. Subsequent western blot analysis with the indicated antibodies demonstrated that exogenous LGALS3BP-FLAG coimmunoprecipitated with endogenous GALNT6 in ZR-75-1 cells (Fig. 1A). Conversely, it was confirmed that GALNT6-FLAG coimmunoprecipitated with endogenous LGALS3BP in HCC1806 cells, which express low levels of GALNT6 (Fig. 1B). Notably, the ~75-kDa band of *O*-glycosylation of coimmunoprecipitated LGALS3BP-FLAG with endogenous GALNT6 was observed by VVA lectin blot analysis (Fig. 1A). By contrast, the ~90-kDa band of *O*-glycosylated LGALS3BP when GALNT6-FLAG was exogenously overexpressed was observed by VVA lectin blot analysis (Fig. 1B). These findings suggest that GALNT6 interacts with and *O*-glycosylates LGALS3BP in breast cancer cells.

To further validate the GALNT6-LGALS3BP interaction, the subcellular localization of these proteins in breast cancer cells was examined by immunocytochemistry. Since GALNT6 is reportedly localized in the Golgi apparatus of breast cancer cells (10,17) and LGALS3BP is reported to be a

Table I. 2DICAL analysis for GALNT6-binding proteins in GALNT6-HA-expressing HeLa cells vs. mock-HeLa cells.

Protein name	Expected value	Peptide sequence
BANF1	6.E-09	HRDFVAEPMGEKPVGSLAGIGEVLGK
BANF1	5.E-08	DFVAEPMGEKPVGSLAGIGEVLGK
TPP1	8.E-08	LYQQHGAGLFDVTR
GALNT6	4.E-07	NSQVPKDEEWELAQDQLIR
KPNB1	4.E-07	VLANPGNSQVAR
VIM	4.E-06	SLYASSPGGVYATR
GALNT6	9.E-06	LAEVWMDSYKK
VIM	1.E-05	LQDEIQNMKEEMAR
TPP1	1.E-05	LFGGNFAHQASVAR
JUP	2.E-05	ALMGSPQLVAAVVR
VIM	2.E-05	NLQEAEEWYK
VIM	9.E-05	ILLAELEQLK
JUP	0.00011	AAMIVNQLSK
JUP	0.00023	LLNDEDPVVVTK
TPP1	0.00028	ILSGRPPLGFLNPR
JUP	0.00031	EGLLAIFK
GALNT6	0.00044	SFGDISER
LGALS3BP	0.00066	AVDTWSWGER
LGALS3BP	0.00075	SDLAVPSELALLK
KPNB1	0.0025	WLAIDANAR
IPO7	0.0026	AIFQTIQNR
LGALS3BP	0.0031	ASHEEVEGLVEK
JUP	0.0059	LAEPSQLLK
BANF1	0.0067	KDEDLFR
KPNB1	0.008	VAAGLQIK
BHLHA9	0.024	GAPGLGLTAR
SCFD1	0.027	IMSKTTLDK
LGALS1	0.029	SFVLNLGK
JUP	0.039	SGGIPALVR
LGALS3BP	0.045	VEIFYR

2DICAL, 2-dimensional image-converted analysis of liquid chromatography-mass spectrometry; GALNT6, polypeptide N-acetylgalactosami nyltransferase 6; LGALS3BP, lectin galactoside-binding soluble 3 binding protein.

heavy glycosylated secreted protein (21-24), their colocalization in the Golgi apparatus of cancer cells was investigated. Both LGALS3BP-FLAG and GALNT6-HA were clearly observed in the Golgi apparatus in HeLa cells, as evaluated by the Golgi marker Golgi-58k (Fig. 1C). Moreover, it was confirmed that stably expressed LGALS3BP-FLAG colocalized with endogenous GALNT6 in the Golgi apparatus in ZR-75-1 cells (Fig. 1D), which suggests that GALNT6 interacts and colocalizes with LGALS3BP in the Golgi apparatus in breast cancer cells.

Effects of GALNT6 on the secretion and O-glycosylation of LGALS3BP. As LGALS3BP is reported to be a secreted galectin-3 ligand glycoprotein in several tumors, including breast cancer (21-25,31,32), the effect of GALNT6-dependent LGALS3BP *O*-glycosylation on LGALS3BP secretion was examined by VVA lectin and western blot analyses. It was confirmed that both GALNT6 WT-HA and the enzyme-dead GALNT6 H271D-HA mutant interacted with LGALS3BP-FLAG in 293T cells (Fig. S3A). However, overexpression of GALNT6 WT-HA, but not GALNT6 H271D-HA, induced the *O*-glycosylation of LGALS3BP-FLAG in the supernatant of transfected HeLa cells (Fig. 2A).

To further validate the results mentioned above, the effects of siRNA-mediated *GALNT6* knockdown on the *O*-glycosylation and secretion of LGALS3BP in the ZR-75-1, BT-20 and SK-BR-3 cell lines were examined by immunoblotting and ELISA. As GALNT6 exhibits the highest structural and amino acid sequence similarity with GALNT3 among GALNT family members, we first examined the specificity of *GALNT6* knockdown on *GALNT3* expression in BT-20 cells by qPCR. The results demonstrated that *GALNT6* knockdown does not affect *GALNT3* expression at the transcriptional level (Fig. S3B). Subsequently, immunoblotting and ELISA demonstrated that silencing *GALNT6* markedly reduced both the intracellular and extracellular release of LGALS3BP into the culture supernatant of ZR-75-1

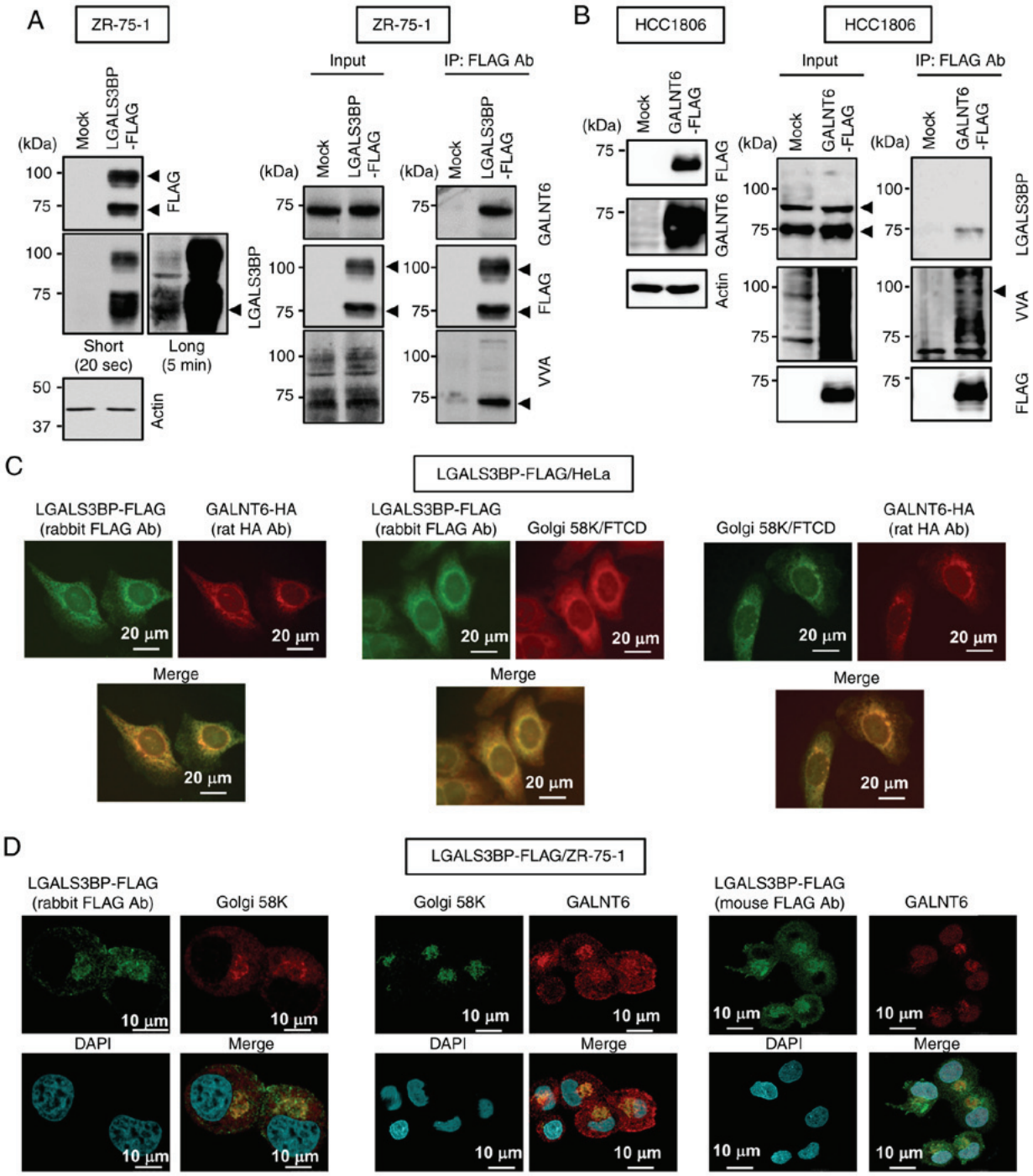

Figure 1. GALNT6 interacts with and *O*-glycosylates LGALS3BP. (A) Immunoblotting of ZR-75-1 cells stably expressing Mock or LGALS3BP-FLAG vectors was performed using the indicated antibodies. The levels of LGALS3BP were analyzed after a short exposure (20 sec) and long exposure (5 min) (left). Cell lysates were immunoprecipitated with anti-FLAG affinity gel and analyzed by immunoblotting using the indicated antibodies and VVA-lectin (right). Arrowheads, LGALS3BP protein. (B) Immunoblotting of HCC1806 cells stably expressing Mock vector and GALNT6-FLAG was performed using the indicated antibodies (left). Cell lysates were immunoprecipitated with anti-FLAG affinity gel. Immunoblotting was performed using the indicated antibodies and VVA-lectin (right). (C and D) GALNT6 colocalizes with LGALS3BP in the Golgi apparatus of cancer cells. (C) HeLa cells stably expressing LGALS3BP-FLAG were transfected with the GALNT6-HA expression plasmid vector. After 24 h, the cells were fixed and subjected to immunofluorescence analysis using the indicated antibodies. (D) ZR-75-1 cells stably expressing LGALS3BP-FLAG were fixed and subjected to immunofluorescence analysis using the mouse FLAG, rabbit GALNT6 and Golgi 58K antibodies, respectively. Nuclei were visualized with DAPI. GALNT6, polypeptide N-acetylgalactosaminyltransferase 6; LGALS3BP, lectin galactoside-binding soluble 3 binding protein; VVA, *Vicia villosa* agglutinin.

(Fig. 2B and E), BT-20 (Fig. 2C and F) and SK-BR-3 (Fig. 2D and G) cells, compared with siEGFP-treated cells. In addition, it was confirmed that the knockdown of *GALNT6* did not affect *LGALS3BP* expression at the transcriptional level in ZR-75-1 cells (Fig. S3C). It was further confirmed that degradation of the LGALS3BP protein was still observed in GALNT6-depleted cells, despite the presence of MG132 (Fig. S3D). These data suggest that the reduction of GALNT6-mediated *O*-glycosylation may cause degradation of the LGALS3BP protein through a

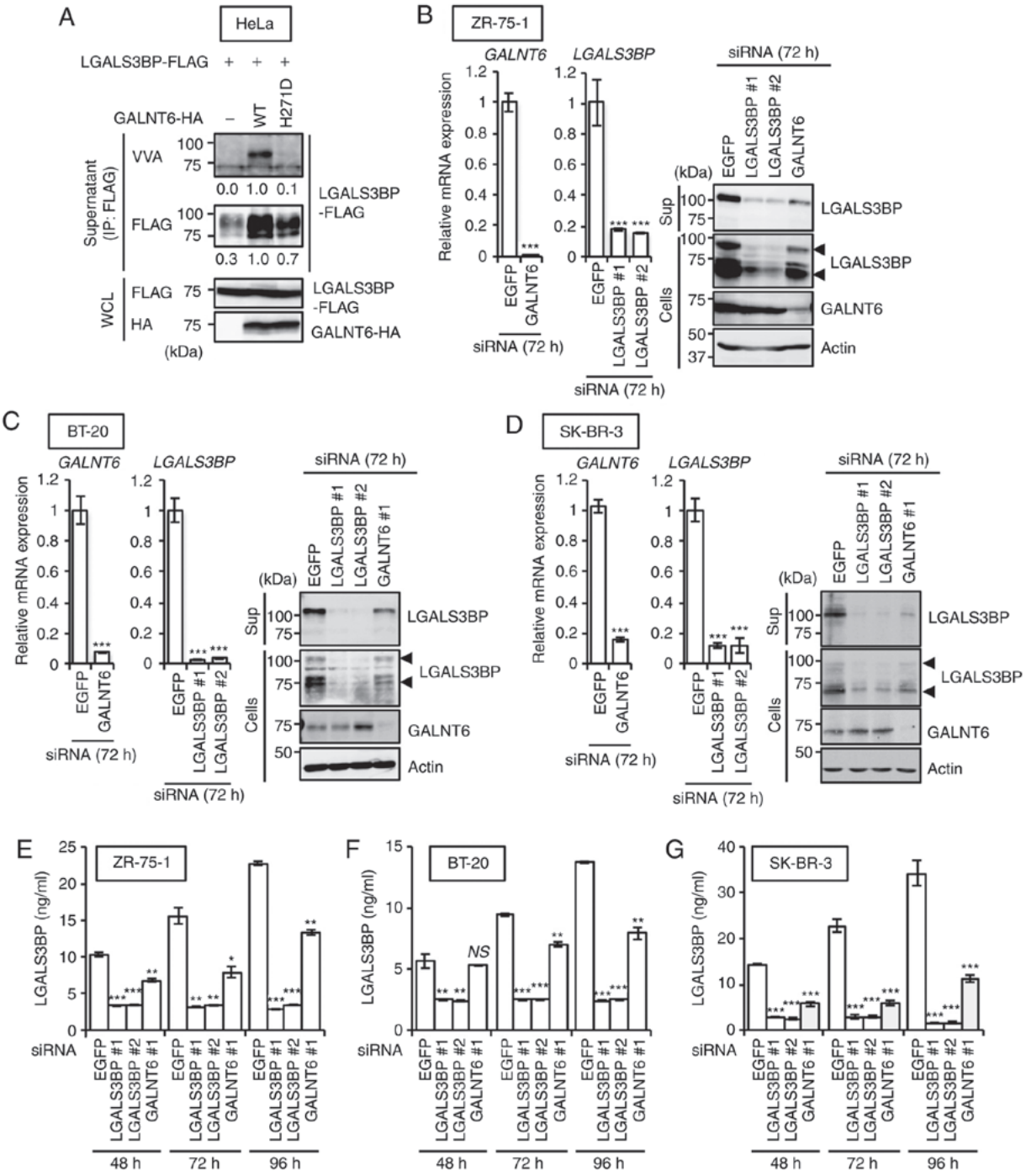

Figure 2. Roles of GALNT6 in the secretion and *O*-glycosylation of LGALS3BP. (A) GALNT6-HA (WT or the enzyme-dead H271D mutant) stably transfected HeLa cells were transfected with the LGALS3BP-FLAG expression plasmid vector. After 72 h, cell supernatants and cell lysates were harvested and immunoprecipitated with anti-FLAG affinity gel. Then, immunoblotting analyses were performed using the indicated antibodies and VVA-lectin. The band densities on the immunoblots are expressed relative to those of cells cotransfected with the LGALS3BP-FLAG and GALNT6 WT-HA expression plasmids, which were defined as 1.0. (B-D) The human breast cancer cell lines (B) ZR-75-1, (C) BT-20 and (D) SK-BR-3 were transfected with EGFP, GALNT6 #1, LGALS3BP #1 or LGALS3BP #2 siRNA. The *GALNT6* and *LGALS3BP* mRNA expression levels were evaluated by quantitative PCR at 72 h after transfection. The levels were expressed relative to those in EGFP siRNA-transfected cells, which were defined as 1.0 (left). The protein levels of LGALS3BP, GALNT6 and actin in the extracellular (Sup: Acetone precipitation) or intracellular (Cells) compartment at 72 h after transfection were determined by immunoblot analysis (right). The data are presented as the means ± standard deviation of three independent experiments (***P<0.001 vs. EGFP siRNA-transfected cells). (E-G) The LGALS3BP protein levels in the culture supernatants of (E) ZR-75-1, (F) BT-20 and (G) SK-BR-3 cells at 48, 72 and 96 h after transfection were determined by LGALS3BP ELISA (Materials and methods). The data are presented at the means ± standard deviation of three independent experiments (**P<0.01, ***P<0.001 vs. EGFP siRNA-transfected cells in each time). NS, not significant. GALNT6, polypeptide N-acetylgalactosaminyltransferase 6; LGALS3BP, lectin galactoside-binding soluble 3 binding protein; WT, wild-type; VVA, *Vicia villosa* agglutinin; WCL, whole-cell lysates; EGFP, enhanced green fluorescent protein.

proteasome-independent proteolysis pathway. Therefore, GALNT6 may regulate LGALS3BP protein stabilization through *O*-glycosylation in breast cancer cells.

Oncogenic effects of the GALNT6-LGALS3BP axis on the proliferation of breast cancer cells. We then sought to investigate the effect of GALNT6 and LGALS3BP on the proliferation

of breast cancer cells. siRNAs were first used to knock down endogenous GALNT6 and LGALS3BP expression in ZR-75-1, BT-20 and SK-BR-3 cells. Silencing of *GALNT6* and *LGALS3BP* inhibited the proliferation of ZR-75-1, BT-20 and SK-BR-3 cells (Fig. 3A) from 72 h after each siRNA transfection. Conversely, stable expression of LGALS3BP-FLAG in ZR-75-1 cells led to marked enhancement of cell growth compared with that in mock-transfected ZR-75-1 cells from 48 h after seeding (Fig. 3B). Subsequently, it was hypothesized that GALNT6 overexpression enhances the release of *O*-glycosylated LGALS3BP from breast cancer cells, thereby promoting the proliferation of these cells. Therefore, we next investigated the effect of soluble LGALS3BP on cell proliferation in breast cancer cell lines. We further analyzed cell proliferation in breast cancer cell lines using conditioned medium (CM) from LGALS3BP-FLAG-overexpressing (LGAL3SBP$^+$) and GALNT6-HA-overexpressing (GALNT6 WT$^+$) HeLa or 293T cells. Treatment with CM from LGAL3SBP$^+$ HeLa cells significantly promoted HCC1806 cell proliferation (Fig. 3C). Notably, CM from LGAL3SBP$^+$/GALNT6 WT$^+$ HeLa and 293T cells significantly enhanced the proliferation of HCC1806 cells in a time-dependent manner compared with the effect of CM from LGAL3SBP$^+$/GALNT6$^-$ or LGAL3SBP$^+$/GALNT6 H271D$^+$ HeLa and 293T cells (Fig. 3C and D). These findings indicate that the *O*-glycosylation of LGALS3BP by GALNT6 is crucial for the enhancement of breast cancer cell proliferation.

The carboxyl-terminal region of LGALS3BP regulates GALNT6-dependent LGALS3BP O-glycosylation and release. To investigate the detailed biological significance of GALNT6-dependent LGALS3BP *O*-glycosylation, we first attempted to determine the critical region(s) required for the *O*-glycosylation and extracellular release of LGALS3BP. Accumulating functional and structural studies have demonstrated that the LGALS3BP protein contains an N-terminal signal sequence, a scavenger receptor cysteine-rich (SRCR) domain for protein-protein interaction, and a BTB and C-terminal Kelch (BACK) domain for interaction with the Cullin3 ubiquitin ligase complex and homo-oligomerization (Fig. 4A) (21,22,36,37). As the function of the C-terminal region of LGALS3BP remains unclear, we focused on this region. Plasmids expressing LGALS3BP C-terminal region deletion mutants [Del-1 (1-538) and Del-2 (1-560) (Fig. 4A)] were generated and both mutants were first cotransfected independently with GALNT6-HA into 293T cells. Next, immunoprecipitation with an anti-FLAG antibody followed by immunoblotting with the indicated antibodies and VVA lectin blot analyses were performed. Both LGALS3BP deletion mutants interacted with GALNT6-HA and were *O*-glycosylated in the intracellular fraction of 293T cells (Fig. 4B). Importantly, extracellular release of LGALS3BP was not observed in the supernatant fraction of the cells transfected with both LGALS3BP deletion mutants and GALNT6-HA (Fig. 4B), indicating that the region between amino acids 561 and 585 of LGALS3BP is the minimal requirement for the extracellular release of LGALS3BP. Moreover, the band of *O*-glycosylated LGAL3SBP was observed in the supernatant from only the cells transfected with full-length LGALS3BP and GALNT6-HA by VVA lectin blot analysis (Fig. 4B).

The region(s) required for GALNT6-dependent LGALS3BP *O*-glycosylation were next investigated. As shown in Fig. 4B, the GALNT6-dependent *O*-glycosylation level of Del-1 and Del-2 determined by VVA in the intracellular fraction (cells) was obviously reduced (60%) compared with that of WT, as indicated by the arrowheads. This result indicates that both the regions between amino acids 1-560 and 561-585 may be required for GALNT6-dependent LGALS3BP *O*-glycosylation. Therefore, we first focused on the Del-2 mutant (amino acids 1-560) of LGALS3BP to identify GALNT6-dependent *O*-glycosylation sites. Because the Del-2 region contains several candidate serine and threonine residues for *O*-glycosylation, which are highly conserved among several species (Fig. S4), Del-2 mutant constructs were prepared, in which each of these candidate residues was separately substituted with alanine (Fig. 4C). Notably, Mut-4 (S555A/T556A) markedly reduced GALNT6-dependent *O*-glycosylation of Del-2 (Fig. 4D). Next, to further narrow down the GALNT6-dependent *O*-glycosylation site(s) within Del-2 region, Mut-6 (S555A) and Mut-7 (T556A) constructs were generated (Fig. 4C). It was confirmed that Mut-7 (T556A), as well as Mut-4 (S555A/T556A), mostly abolished GALNT6-dependent *O*-glycosylation of LGALS3BP (Fig. 4E), suggesting that T556 is a strong candidate site for GALNT6-dependent *O*-glycosylation of LGALS3BP.

Finally, we attempted to validate this result using the T556A mutant plasmid vector from the full-length LGALS3BP sequence. Unexpectedly, a strong band representing GALNT6-dependent LGALS3BP *O*-glycosylation was observed in the supernatant fraction from GALNT6 WT-transfected cells via VVA lectin blot analysis (Fig. 4F), suggesting that the region encompassing amino acids 561-585 contains at least one other site putatively *O*-glycosylated by GALNT6. Furthermore, a slight reduction of the LGALS3BP protein secretion level was observed in the supernatant from both LGALS3BP-T556A-and mock-transfected cells, suggesting that, in addition to T556, at least one other putative GALNT6-dependent *O*-glycosylation site may be located within the region encompassing amino acids 561-585 of LGALS3BP.

Identification of GALNT6-dependent LGALS3BP O-glycosylation, which is required for LGALS3BP secretion. We further attempted to narrow down the site(s) required for additional *O*-glycosylation site(s) of secreted LGALS3BP within the region encompassing amino acids 561-585, and the first focus was on T571 (Fig. 5A). The results demonstrated that the double alanine substitution of T556/T571 (T556A/T571A) markedly attenuated the levels of *O*-glycosylation and extracellular release of LGALS3BP compared with those of the full-length WT protein in GALNT6-WT-transfected HeLa cells (Fig. 5B). Moreover, T556A/T571A resulted in substantial attenuation compared with that resulting from the T571A mutation (Fig. S5A). These results indicate that T556 and T571 are strong candidate GALNT6-dependent *O*-glycosylation sites critical for extracellular release of LGALS3BP.

Three candidate sites (T579, S581 and S582) in the distal region of LGALS3BP (amino acids 572-585) were examined and T579A, S581A and S582A mutants of LGALS3BP were generated (Fig. 5C). GALNT6-dependent *O*-glycosylation of

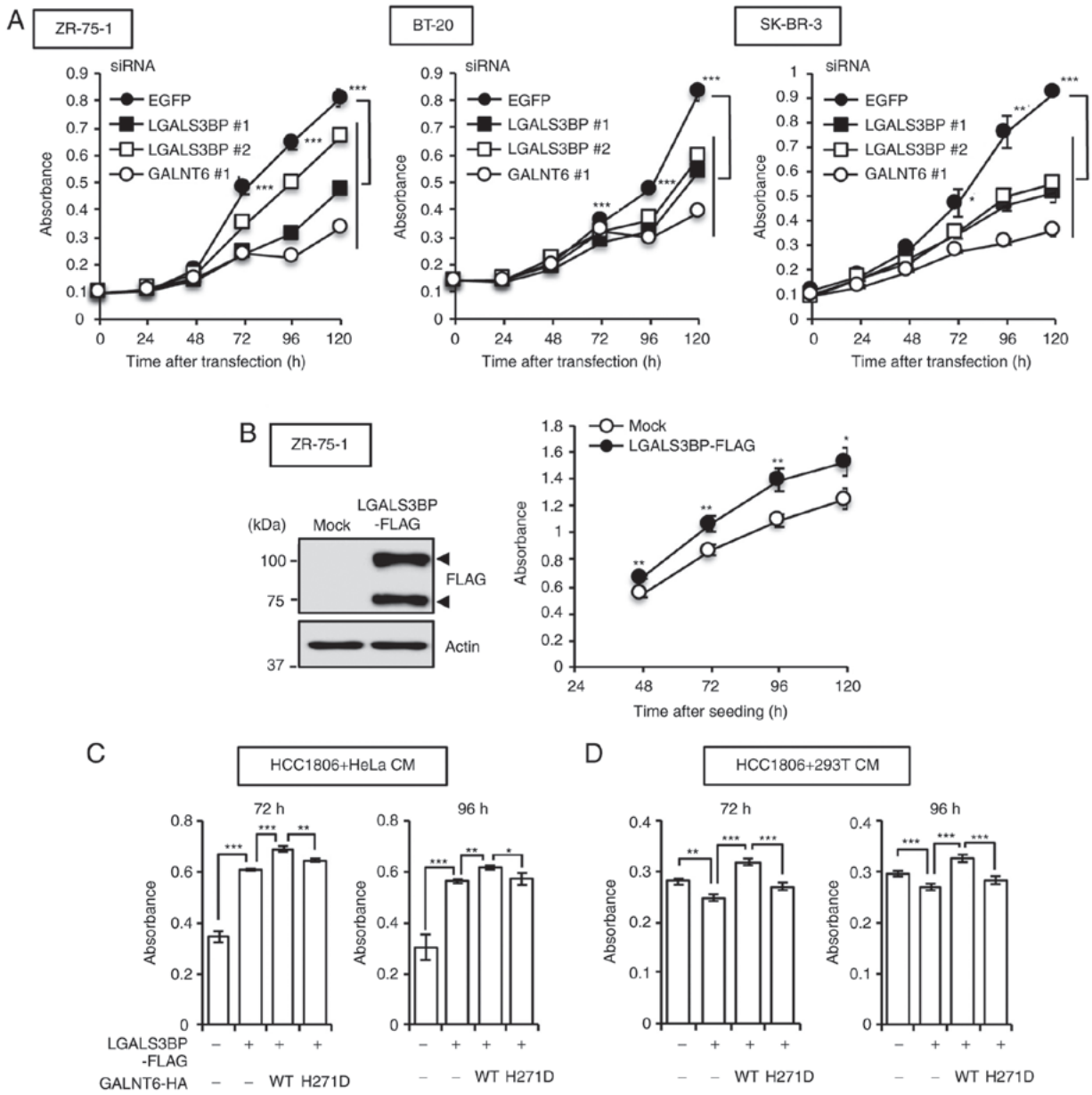

Figure 3. Effect of GALNT6-dependent LGALS3BP *O*-glycosylation on cell growth. (A) Cell proliferation following transfection with EGFP, GALNT6 #1, LGALS3BP #1 or LGALS3BP #2 siRNA was assessed in ZR-75-1 (left), BT-20 (middle) and SK-BR-3 (right) cells at 0, 24, 48, 72, 96 or 120 h after transfection via a WST-8 assay. The data are presented as the means ± standard deviation of three independent experiments (*P<0.05, **P<0.01, ***P<0.001 vs. EGFP siRNA-transfected cells). (B) The proliferation of ZR-75-1 cells stably expressing Mock or LGALS3BP-FLAG vectors (left) was assessed at 48, 72, 96 and 120 h after seeding via a WST-8 assay (right). The data are presented as the means ± standard deviation of three independent experiments (*P<0.05, **P<0.01 vs. mock-transfected ZR-75-1 cells). (C) HeLa or (D) 293T cells were cotransfected with the LGALS3BP-FLAG and GALNT6-HA expression plasmid vectors. After 24 h, the medium was replaced with (C) 1% FBS/RPMI or (D) 2% FBS/RPMI medium, and CM was harvested at 72 h after the medium change. Next, the medium of HCC1806 cells was replaced with CM from (C) HeLa or (D) 293T cells, and proliferation was assessed at 72 and 96 h after the medium change via a WST-8 assay. The data are presented as the means ± standard deviation of three independent experiments (*P<0.05, **P<0.01, ***P<0.001). NS, not significant; CM, conditioned medium; GALNT6, polypeptide N-acetylgalactosaminyltransferase 6; LGALS3BP, lectin galactoside-binding soluble 3 binding protein; EGFP, enhanced green fluorescent protein.

LGALS3BP S582A was most significantly attenuated compared with that of LGALS3BP WT in GALNT6-WT-transfected HeLa cells (Fig. 5D and Fig. S5B). More importantly, among these mutants, only LGALS3BP S582A-FLAG exhibited a significant decrease of GALNT6-dependent *O*-glycosylation in the supernatant fraction compared with that of LGALS3BP WT in HeLa cells (Fig. 5D and Fig. S5B). Accordingly, the results mentioned above were validated using a triple Ala substitution construct (T556A/T571A/T582A), and it was observed that T556A/T571A/T582A resulted in the most significant decrease in GALNT6-dependent *O*-glycosylation and secretion compared with that of LGALS3BP WT in HeLa cells (Fig. 5E and Fig. S5C). These findings suggest the possibility that T556, T571 and S582 are crucial for GALNT6-mediated *O*-glycosylation and secretion of LGALS3BP, although further analysis of the involvement of GALNT6-mediated *O*-glycosylation in the secretion of LGALS3BP in breast cancer cells is required.

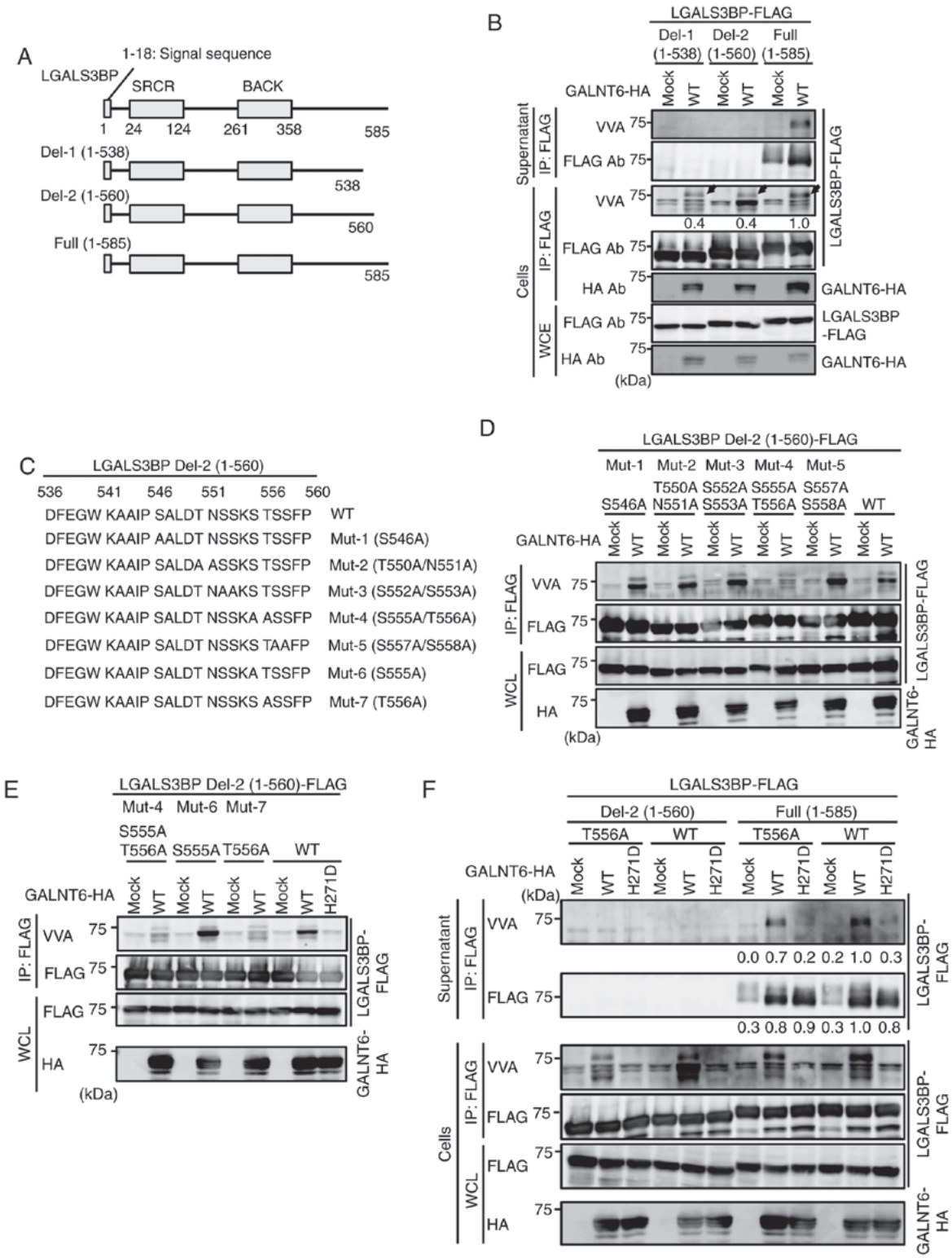

Figure 4. The carboxyl-terminal region of LGALS3BP regulates GALNT6-dependent LGALS3BP *O*-glycosylation and release. (A) Schematic diagram of LGALS3BP and deletion mutants (Del-1, Del-2 and Full). (B) 293T cells were cotransfected with the LGALS3BP deletion mutant-FLAG (Del-1, Del-2 or Full) and GALNT6-HA expression plasmid vectors. After 72 h, cell supernatants and cell lysates (Cells) were harvested and immunoprecipitated with anti-FLAG affinity gel. Immunoblotting was performed using the indicated antibodies and VVA-lectin. Arrowheads, potential *O*-glycosylation of intracellular LGALS3BP-FLAG protein. (C) Schematic diagram of the LGALS3BP Del-2 (1-560) point mutants (Mut-1, -2, -3, -4, -5, -6 and -7). (D) 293T cells were cotransfected with the LGALS3BP Del-2 (1-560) point mutant-FLAG (Mut-1, -2, -3, -4 or -5) or the WT (1-560)-FLAG expression plasmid and GALNT6-HA expression plasmids. After 72 h, cell lysates were harvested and immunoprecipitated with anti-FLAG affinity gel. (E) 293T cells were cotransfected with either the LGALS3BP Del-2 (1-560) point mutant-FLAG (Mut-4, -6 or -7) or the WT (1-560)-FLAG expression plasmid and GALNT6-HA expression plasmids. After 72 h, cell lysates were harvested and immunoprecipitated with anti-FLAG affinity gel. (F) 293T cells were cotransfected with either the LGALS3BP Del-2 (1-560) T556A, Del-2 (1-560) WT, full-length T556A or full-length WT-FLAG and the GALNT6-HA expression plasmid vectors. After 72 h, cell supernatants and cell lysates (Cells) were harvested and immunoprecipitated with anti-FLAG affinity gel. The band densities on the immunoblot are expressed relative to those of cells cotransfected with the LGALS3BP full-length WT-FLAG and GALNT6 WT-HA expression plasmid vectors, which were defined as 1.0. GALNT6, polypeptide N-acetylgalactosaminyltransferase 6; LGALS3BP, lectin galactoside-binding soluble 3 binding protein; WCL, whole-cell lysates; SRCR, scavenger receptor cysteine-rich; BACK, BTB and C-terminal Kelch; WT, wild-type; VVA, *Vicia villosa* agglutinin.

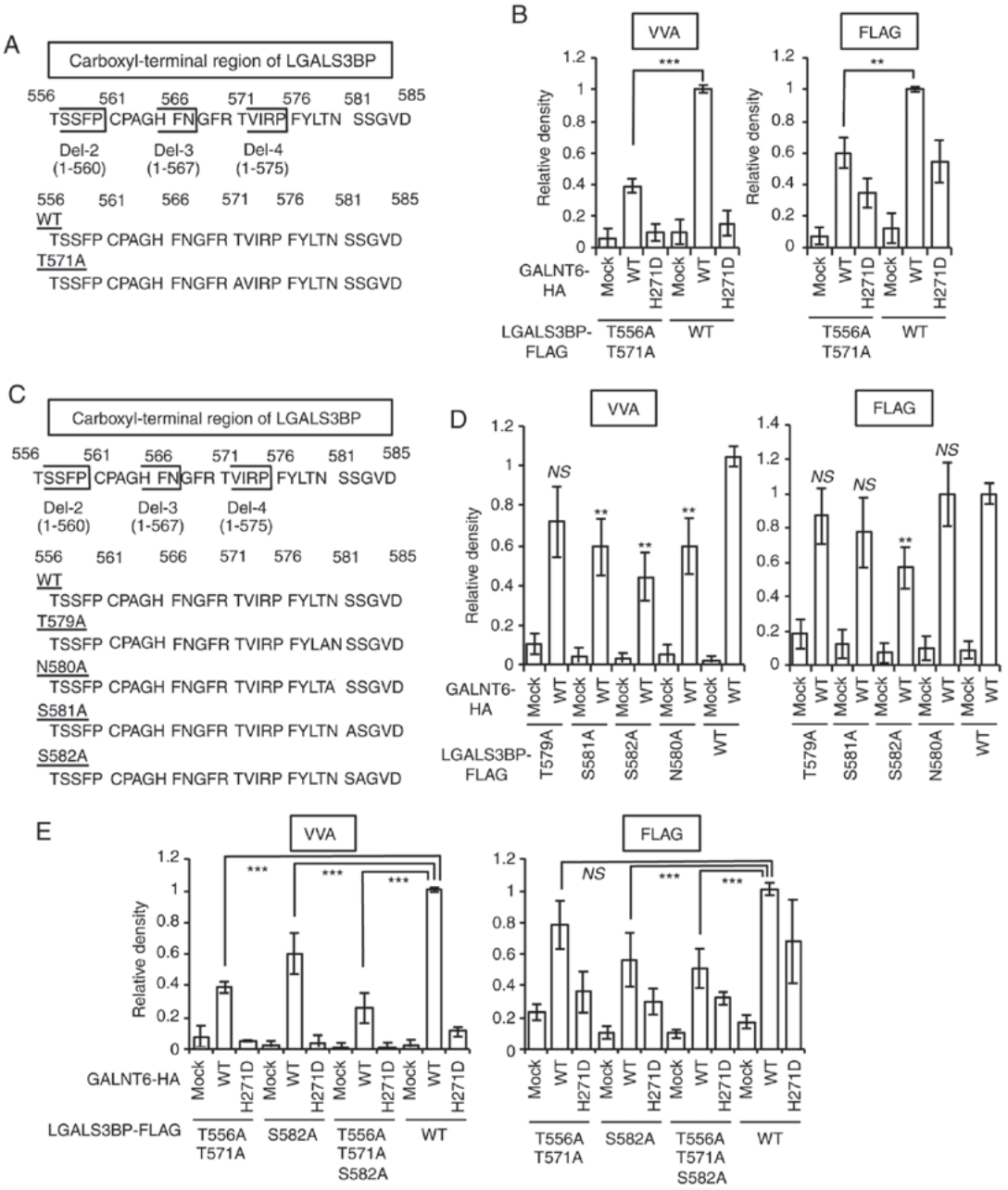

Figure 5. Identification of GALNT6-dependent LGALS3BP *O*-glycosylation, which is required for LGALS3BP secretion. (A) Schematic diagram of the LGALS3BP T571A point mutant. (B) HeLa cells were cotransfected with either the LGALS3BP T556A/T571A or WT-FLAG and the GALNT6-HA expression plasmid vectors. After 72 h, cell supernatants and cell lysates were harvested and immunoprecipitated with anti-FLAG affinity gel. The band densities on the immunoblot are expressed relative to those of cells cotransfected with the LGALS3BP WT-FLAG and GALNT6 WT-HA expression plasmid vectors, which were defined as 1.0. The data are presented as the means ± standard deviation of three independent experiments (***P<0.001). (C) Schematic diagram of the LGALS3BP T579A, S581A and S582A and N580A (a negative control site for *O*-glycosylation; a potential N-glycosylation site) point mutants. (D and E) HeLa cells were cotransfected with the LGALS3BP point mutant-FLAG and GALNT6-HA expression plasmids. After 72 h, cell supernatants were harvested and immunoprecipitated with anti-FLAG affinity gel. The band densities on the immunoblot are expressed relative to those of cells cotransfected with the LGALS3BP WT-FLAG and GALNT6 WT-HA expression plasmid vectors, which were defined as 1.0. The data are presented at the means ± standard deviation of three independent experiments (**P<0.001, ***P<0.001; NS, not significant)

Subsequently, to validate the *O*-glycosylation of LGALS3BP by GALNT6, an *in vitro* GalNAc transferase assay was performed. GALNT6 *O*-glycosylated LGALS3BP WT peptide (568-585 amino acids) in a dose-dependent manner (Fig. 5F). However, GALNT6-dependent *O*-glycosylation of LGALS3BP mutant peptides (T571A and S582A) was significantly attenuated. Notably, GALNT6-dependent *O*-glycosylation of the LGALS3BP double-mutant peptide (T571A/S582A) was almost abolished. Taken together, these findings strongly suggest that GALNT6-dependent *O*-glycosylation of LGALS3BP at T556, T571 and S582 is indispensable for the extracellular release of LGALS3BP in cancer cells.

Autocrine growth-promoting effect of GALNT6-O-glycosylated LGALS3BP. Finally, to investigate the significance of the secretion of *O*-glycosylated LGALS3BP, the growth-promoting effect of CM from LGALS3BP (T556A/T571A/S582A)- and GALNT6 (WT or H271D)-overexpressing cells was evaluated.

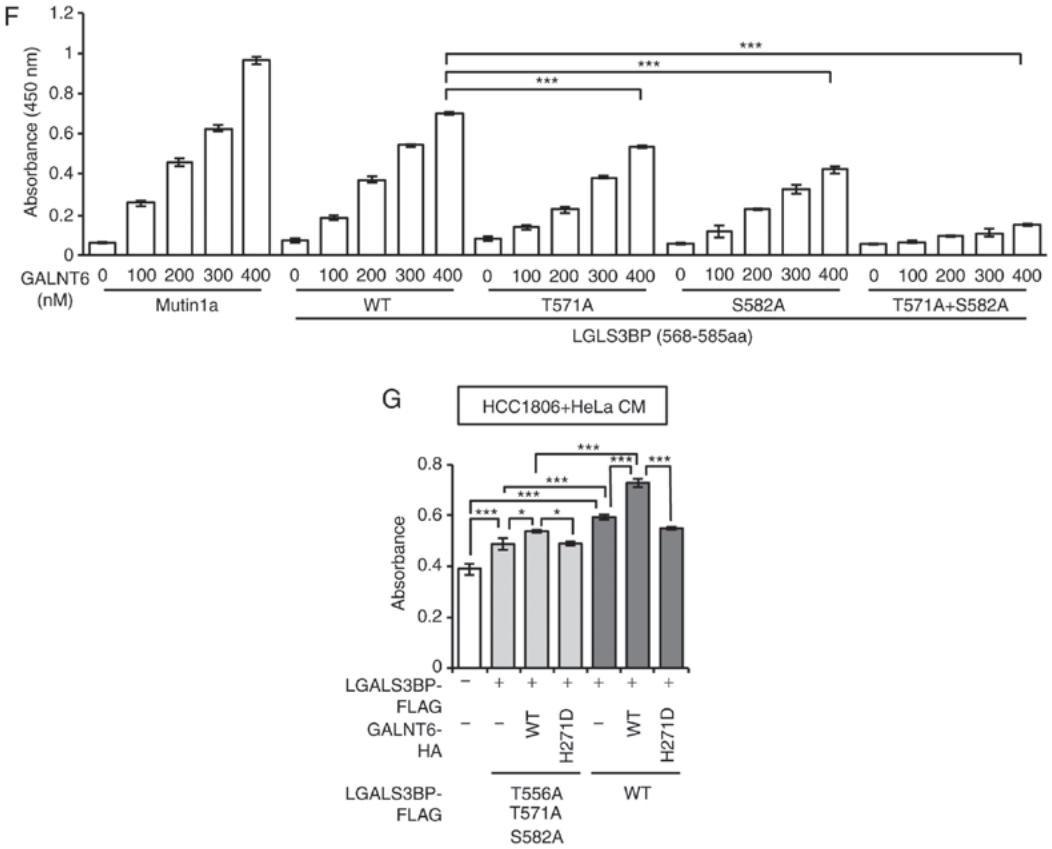

Figure 5. Continued. Identification of GALNT6-dependent LGALS3BP *O*-glycosylation, which is required for LGALS3BP secretion. (F) GALNT6 *O*-glycosylates the LGALS3BP protein *in vitro*. *In vitro O*-glycosylation of the LGALS3BP-WT, T571A, S582A and T571A+ S582A peptides (amino acids 568-585) by WT-GALNT6 recombinant proteins after a 16 h reaction. The data are presented as the means ± standard deviation of three independent experiments (***P<0.001). (G) HeLa cells were cotransfected with the LGALS3BP-FLAG and GALNT6-HA expression plasmids. After 24 h, the medium was replaced with 1% FBS/RPMI medium, and the CM was harvested at 72 h after the medium change. Next, the medium of the HCC1806 cells was replaced with HeLa cell CM, and cellular proliferation was determined using a WST-8 assay at 96 h after the medium change. The data are presented as the means ± standard deviation of three independent experiments (*P<0.05, **P<0.01, ***P<0.001). NS, not significant; GALNT6, polypeptide N-acetylgalactosaminyltransferase 6; LGALS3BP, lectin galactoside-binding soluble 3 binding protein; WT, wild-type; CM, conditioned medium; VVA, *Vicia villosa* agglutinin.

CM was transferred to HCC1806 cells and then a cell proliferation assay was performed. The promoting effect of CM derived from LGAL3SBP T556A/T571A/S582A/GALNT6 WT+ HeLa cells was significantly attenuated compared with that of CM from LGAL3SBP WT/GALNT6 WT+ HeLa cells (Fig. 5G). These findings suggest that *O*-glycosylation at T556, T571 and S582 of LGALS3BP is crucial for the release of LGALS3BP and its autocrine growth-promoting effects in breast cancer cells. Taken together, these findings demonstrated that the GALNT6-LGALS3BP axis regulates mammary carcinogenesis through GALNT6-dependent LGALS3BP *O*-glycosylation and release.

Discussion

In the present study, LGALS3BP was identified as a novel substrate of GALNT6 in breast cancer cells. Although accumulating studies have revealed the significance of each protein in breast cancer (10,17,19,21-23,24-27), their interaction and regulation have yet to be elucidated. To the best of our knowledge, the present study is the first to demonstrate that overexpressed GALNT6 colocalizes with and *O*-glycosylates LGALS3BP in the Golgi apparatus, thereby enhancing the extracellular release of *O*-glycosylated LGALS3BP from breast cancer cells, which then acts in an autocrine manner to promote breast cancer cell growth. Previous studies have demonstrated that LGALS3BP is overexpressed in and secreted by several tumor tissues, including breast cancer tissues (23-32). Several functional and structural studies indicate that the LGALS3BP protein is potentially asparagine (N-) linked glycosylated, but not *O*-linked glycosylated (36,37). However, the recombinant LGALS3BP protein used in these studies was generated from embryonic kidney cells that do not express GALNT6. Therefore, the present findings were the first to demonstrate that LGALS3BP is *O*-linked glycosylated by GALNT6, which is overexpressed in breast cancer cells. More importantly, through biochemical analysis using deletion mutant and alanine mutant constructs, three GALNT6-mediated *O*-glycosylation sites (T556, T571 and S582) were identified on the LGALS3BP protein, and they are indispensable for its secretion and growth-promoting autocrine activity. When GALNT6 expression was knocked down in ZR-75-1, BT-20 and SK-BR-3 breast cancer cells, the *O*-glycosylation and flow of endogenous LGALS3BP were noticeably decreased, suggesting that GALNT6 is crucial for the *O*-glycosylation and secretion of endogenous LGALS3BP in breast cancer cells. Furthermore, it was demonstrated that treatment with CM from LGAL3SBP+GALNT6+ HeLa

cells significantly promoted HCC1806 cell proliferation (Fig. 3C). On the other hand, the effect of LGALS3BP in CM from 293T cells on cell proliferation was found to be mildly suppressive for HCC1806 cells (Fig. 3D). As the endogenous LGAL3BP is not GALNT6-mediated *O*-glycosylated in 293T cells (Fig. 4B), these findings suggest the possibility that the dominant-negative effect of non-*O*-glycosylated LGALS3BP derived from 293T cells may result from interference with its cell proliferative function in HCC1806 cells.

Furthermore, the ~75-kDa band of *O*-glycosylated LGALS3BP by endogenous GALNT6 (Fig. 1A) was detected by VVA lectin blot analysis, even when LGALS3BP-FLAG was overexpressed in any cells. By contrast, the higher (~90 kDa) band of *O*-glycosylated LGALS3BP was observed when GALNT6-FLAG or -HA was exogenously overexpressed (Figs. 1B and 2A). As GALNT6 catalyzes the transfer of GalNAc to serine or threonine residues during the first step of *O*-linked protein glycosylation, the aberrant structure of glycan chains that are covalently attached to LGALS3BP may occur due to exogenous GALNT6 overexpression, thereby not extending glycan chain in breast cancer cells, although further analyses are require to clarify this issue.

Previous reports demonstrated that GALNT6 *O*-glycosylates several cancer-related proteins as substrates, including MUC1, fibronectin, MUC4, GRP78 and ER, in order to stabilize these proteins in cancer cells (10,17-19). Notably, GALNT6 is also likely to be required for the stabilization of the endogenous LGALS3BP protein via *O*-glycosylation, as knockdown of *GALNT6* reduced intracellular LGALS3BP expression at the protein level (Fig. 2B) but not at the transcriptional level in breast cancer cells (Fig. S3B). However, no reduction was observed in the total amount of LGALS3BP protein in either LGALS3BP (T556A/T571A/S582A)- or GALNT6 (WT)-overexpressing cells, although we observed *O*-glycosylation of the LGALS3BP protein in both LGALS3BP (T556A/T571A/S582A)- and GALNT6 (WT)-overexpressing cells (Fig. S5C). Taken together, these findings suggest the possibility that another region of LGALS3BP may contain at least one other GALNT6-dependent *O*-glycosylation site for LGALS3BP stability, whereas GALNT6-dependent *O*-glycosylation at T556/T571/S582 is essential for the autocrine growth-promoting activity of LGALS3BP. Further analyses are required to identify the *O*-glycosylation site(s) required for LGALS3BP stability in breast cancer cells.

Finally, the importance of LGALS3BP *O*-glycosylation at T556/T571/S582 to its secretion from cancer cells was considered, as a decrease in *O*-glycosylated LGALS3BP was observed in the supernatant from both LGALS3BP (T556A/T571A/S582A)- and GALNT6 (WT)-overexpressing cells. LGALS3BP released via GALNT6 promoted the proliferation of breast cancer cells (Fig. 5G). It is predicted that soluble LGALS3BP binds to adhesion molecules in the extracellular matrix of tumor cells and regulates adhesion molecule-dependent signaling pathways for oncogenic events. Previous studies demonstrated that LGALS3BP oligomerizes and interacts with galectin-3, the integrin β1 subunit, collagens IV, V and VI, fibronectin and nidogen in the extracellular matrix (38,39). In addition, LGALS3BP regulates integrin-mediated cellular adhesion and promotes cell viability, motility and migration during oncogenic cellular events through the Akt, ERK1/2 and JNK1/2 signaling pathways (40). LGALS3BP *O*-glycosylated by GALNT6 may interact with these adhesion molecules and enhance downstream signaling during oncogenic events, although further analyses are required to fully elucidate the connection between GALNT6 and LGALS3BP in breast cancer cells. Furthermore, a recent study demonstrated that LGALS3BP acts as a centriole- and basal body-associated protein, and LGALS3BP leads to centrosome hypertrophy in cancer cells (41). Accordingly, it may be hypothesized that the intracellular GALNT6-LGALS3BP axis plays a crucial role in regulating the centrosome in breast cancer cells.

Clinically, the diagnostic markers available for breast cancer are not sufficiently sensitive or specific to detect early-stage tumors. Previous studies demonstrated that high serum or tumor tissue levels of LGALS3BP were associated with shorter survival in patients with several types of tumors, including breast cancer (26-32). Moreover, a recent study demonstrated that anti-LGALS3BP antibody blocks LGALS3BP-integrin binding and LGALS3BP-integrin-mediated cellular adhesion, viability and motility (40). These reports and the results of the present study collectively demonstrate that LGALS3BP is a potential prognostic biomarker and therapeutic target for breast cancer. To the best of our knowledge, the present study was the first to demonstrate that a cancer-specific *O*-glycosidase, GALNT6, regulates LGALS3BP secretion to induce its growth-promoting activity via *O*-glycosylation. More importantly, GALNT6 glycosylates a number of cancer-related proteins, including LGALS3BP, regulating the proliferation and metastatic ability of cancer cells, suggesting that a GALNT6-specific inhibitor may be a more attractive anticancer drug for treating breast tumors, compared with LGALS3BP-targeted drugs.

In conclusion, the GALNT6-LGALS3BP axis appears to be crucial for mammary carcinogenesis and may hold promise as a therapeutic target and biomarker for mammary tumors.

Acknowledgements

The authors would like to thank Ms. Hinako Koseki and Ms. Hitomi Kawakami for providing excellent technical support.

Funding

The present study was supported by a grant/research support from the Tokushima Breast Care Clinic and Sagawa Cancer Research Promotion Public Interest Foundation. The study was also supported by the Project for Development of Innovative Research on Cancer Therapeutics (P-DIRECT) (11104836) from the Japan Agency for Medical Research and Development (AMED) and Grants-in-Aid for Scientific Research on Innovative Areas (JP17H06419) and for Young Scientists (B) (JSPS KAKENHI JP16K19052) from the MEXT of Japan. The present study was also supported by the Research Clusters program of Tokushima University.

Availability of data and materials

The data for *GALNT6* mRNA expression (RNA Seq V2 RSEM) in primary invasive breast carcinoma samples were downloaded from TCGA network (http://cancergenome.nih.gov/) (42,43). Kaplan-Meier analyses for breast cancer patients

were downloaded from the Kaplan-Meier plotter (KM plotter) database (http://kmplot.com/analysis/) (44). Breast cancer patients in the KM plotter database were stratified into 'low' and 'high' *GALNT6* mRNA expression groups (Affymetrix ID: 219956_at) based on an autoselected best cutoff value. The datasets used and/or analyzed during the current study are available from the corresponding author on reasonable request.

Authors' contributions

RK performed the GALNT6-LGALS3BP functional analysis experiments, interpreted all data and prepared the draft of the manuscript. TY performed the glycosylation assay, interpreted all data, and the preparation of the draft of the manuscript. YMa performed analyses for TCGA datasets, interpreted all data, and the preparation of the draft of the manuscript. TM performed the screening of GALNT6 binding protein and validation of the GALNT6-LGALS3BP interaction. MO performed the 2DICAL analysis. YMi and MS provided the interpretation of the clinical association data. JHP and YN discussed the interpretation of identification of GALNT6 binding proteins. TK was involved in the conception and design of all studies, the interpretation of the data, and the preparation of the draft and final version of the manuscript. All authors have read and approved the final manuscript.

Ethics approval and consent to participate

All experiments were conducted according to protocols reviewed and approved by the Committee for Safe Handling of Living Modified Organisms at Tokushima University (Permission no. 30-67).

Patient consent for publication

Not applicable.

Competing interests

Jae-Hyun Park is an employee of Cancer Precision Medicine, Inc. Yusuke Nakamura is a stockholder and scientific advisor of OncoTherapy Science, Inc. Toyomasa Katagiri is an external board member and stockholder of OncoTherapy Science, Inc. The remaining authors declare no competing financial interests.

References

1. Tarp MA and Clausen H: Mucin-type O-glycosylation and its potential use in drug and vaccine development. Biochim Biophys Acta 1780: 546-563, 2008.
2. Gill DJ, Clausen H and Bard F: Location, location, location: New insights into O-GalNAc protein glycosylation. Trends Cell Biol 21: 149-158, 2011.
3. Schjoldager KT and Clausen H: Site-specific protein O-glycosylation modulates proprotein processing-deciphering specific functions of the large polypeptide GalNAc-transferase gene family. Biochim Biophys Acta 1820: 2079-2094, 2012.
4. Pinho SS and Reis CA: Glycosylation in cancer: Mechanisms and clinical implications. Nat Rev Cancer 15: 540-555, 2015.
5. Hakomori S: Glycosylation defining cancer malignancy: New wine in an old bottle. Proc Natl Acad Sci USA 99: 10231-10233, 2002.
6. Hussain MR, Hoessli DC and Fang M: N-acetylgalactosaminyltransferases in cancer. Oncotarget 7: 54067-54081, 2016.
7. Berois N, Mazal D, Ubillos L, Trajtenberg F, Nicolas A, Sastre-Garau X, Magdelenat H and Osinaga E: UDP-N-acetyl-D-galactosamine: Polypeptide N-acetylgalactosaminyltransferase-6 as a new immunohistochemical breast cancer marker. J Histochem Cytochem 54: 317-328, 2006.
8. Freire T, Berois N, Sóñora C, Varangot M, Barrios E and Osinaga E: UDP-N-acetyl-D-galactosamine:polypeptide N-acetylgalactosaminyltransferase 6 (ppGalNAc-T6) mRNA as a potential new marker for detection of bone marrow-disseminated breast cancer cells. Int J Cancer 119: 1383-1388, 2006.
9. Patani N, Jiang W and Mokbel K: Prognostic utility of glycosyltransferase expression in breast cancer. Cancer Genomics Proteomics 5: 333-340, 2008.
10. Park JH, Nishidate T, Kijima K, Ohashi T, Takegawa K, Fujikane T, Hirata K, Nakamura Y and Katagiri T: Critical roles of mucin 1 glycosylation by transactivated polypeptide N-acetylg alactosaminyltransferase 6 in mammary carcinogenesis. Cancer Res 70: 2759-2769, 2010.
11. Liesche F, Kölbl AC, Ilmer M, Hutter S, Jeschke U and Andergassen U: Role of N-acetylgalactosaminyltransferase 6 in early tumorigenesis and formation of metastasis. Mol Med Rep 13: 4309-4314, 2016.
12. Lin TC, Chen ST, Huang MC, Huang J, Hsu CL, Juan HF, Lin HH and Chen CH: GALNT6 expression enhances aggressive phenotypes of ovarian cancer cells by regulating EGFR activity. Oncotarget 8: 42588-42601, 2017.
13. Sheta R, Bachvarova M, Plante M, Gregoire J, Renaud MC, Sebastianelli A, Popa I and Bachvarov D: Altered expression of different GalNAc-transferases is associated with disease progression and poor prognosis in women with high-grade serous ovarian cancer. Int J Oncol 51: 1887-1897, 2017.
14. Kitada S, Yamada S, Kuma A, Ouchi S, Tasaki T, Nabeshima A, Noguchi H, Wang KY, Shimajiri S, Nakano R, *et al*: Polypeptide N-acetylgalactosaminyl transferase 3 independently predicts high-grade tumours and poor prognosis in patients with renal cell carcinomas. Br J Cancer 109: 472-481, 2013.
15. Li Z, Yamada S, Wu Y, Wang KY, Liu YP, Uramoto H, Kohno K and Sasaguri Y: Polypeptide N-acetylgalactosaminyltransferase-6 expression independently predicts poor overall survival in patients with lung adenocarcinoma after curative resection. Oncotarget 7: 54463-54473, 2016.
16. Li Z, Yamada S, Inenaga S, Imamura T, Wu Y, Wang KY, Shimajiri S, Nakano R, Izumi H, Kohno K and Sasaguri Y: Polypeptide N-acetylgalactosaminyltransferase 6 expression in pancreatic cancer is an independent prognostic factor indicating better overall survival. Br J Cancer 104: 1882-1889, 2011.
17. Park JH, Katagiri T, Chung S, Kijima K and Nakamura Y: Polypeptide N-acetylgalactosaminyltransferase 6 disrupts mammary acinar morphogenesis through O-glycosylation of fibronectin. Neoplasia 13: 320-326, 2011.
18. Tarhan YE, Kato T, Jang M, Haga Y, Ueda K, Nakamura Y and Park JH: Morphological changes, cadherin switching, and growth suppression in pancreatic cancer by GALNT6 knockdown. Neoplasia 18: 265-272, 2016.
19. Lin J, Chung S, Ueda K, Matsuda K, Nakamura Y and Park JH: GALNT6 stabilizes GRP78 protein by O-glycosylation and enhances its activity to suppress apoptosis under stress condition. Neoplasia 19: 43-53, 2017.
20. Deng B, Tarhan YE, Ueda K, Ren L, Katagiri T, Park JH and Nakamura Y: Critical role of estrogen receptor alpha O-glycosylation by N-acetylgalactosaminyltransferase 6 (GALNT6) in its nuclear localization in breast cancer cells. Neoplasia 20: 1038-1044, 2018.
21. Koths K, Taylor E, Halenbeck R, Casipit C, and Wang A: Cloning and characterization of a human Mac-2-binding protein, a new member of the superfamily defined by the macrophage scavenger receptor cysteine-rich domain. J Biol Chem 268: 14245-14249, 1993.
22. Ullrich A, Sures I, D'Egidio M, Jallal B, Powell TJ, Herbst R, Dreps A, Azam M, Rubinstein M, Natoli C, *et al*: The secreted tumor-associated antigen 90K is a potent immune stimulator. J Biol Chem 269: 18401-18407, 1994.
23. Iacobelli S, Arnò E, D'Orazio A and Coletti G: Detection of antigens recognized by a novel monoclonal antibody in tissue and serum from patients with breast cancer. Cancer Res 46: 3005-3010, 1986.

24. Linsley PS, Horn D, Marquardt H, Brown JP, Hellström I, Hellström KE, Ochs V and Tolentino E: Identification of a novel serum protein secreted by lung carcinoma cells. Biochemistry 25: 2978-2986, 1986.
25. Iacobelli S, Bucci I, D'Egidio M, Giuliani C, Natoli C, Tinari N, Rubistein M and Schlessinger J: Purification and characterization of a 90 kDa protein released from human tumors and tumor cell lines. FEBS Lett 319: 59-65, 1993.
26. Iacobelli S, Sismondi P, Giai M, D'Egidio M, Tinari N, Amatetti C, Di Stefano P and Natoli C: Prognostic value of a novel circulating serum 90K antigen in breast cancer. Br J Cancer 69: 172-176, 1994.
27. Tinari N, Lattanzio R, Querzoli P, Natoli C, Grassadonia A, Alberti S, Hubalek M, Reimer D, Nenci I, Bruzzi P, *et al*: High expression of 90K (Mac-2 BP) is associated with poor survival in node-negative breast cancer patients not receiving adjuvant systemic therapies. Int J Cancer 124: 333-338, 2009.
28. Fornarini B, D'Ambrosio C, Natoli C, Tinari N, Silingardi V and Iacobelli S: Adhesion to 90K (Mac-2 BP) as a mechanism for lymphoma drug resistance in vivo. Blood 96: 3282-3285, 2000.
29. Strizzi L, Muraro R, Vianale G, Natoli C, Talone L, Catalano A, Mutti L, Tassi G and Procopio A: Expression of glycoprotein 90K in human malignant pleural mesothelioma: Correlation with patient survival. J Pathol 197: 218-223, 2002.
30. Marchetti A, Tinari N, Buttitta F, Chella A, Angeletti CA, Sacco R, Mucilli F, Ullrich A and Iacobelli S: Expression of 90K (Mac-2 BP) correlates with distant metastasis and predicts survival in stage I non-small cell lung cancer patients. Cancer Res 62: 2535-2539, 2002.
31. Grassadonia A, Tinari N, Iurisci I, Piccolo E, Cumashi A, Innominato P, D'Egidio M, Natoli C, Piantelli M and Iacobelli S: 90K (Mac-2 BP) and galectins in tumor progression and metastasis. Glycoconj J 19: 551-556, 2002.
32. Grassadonia A, Tinari N, Natoli C, Yahalom G and Iacobelli S: Circulating autoantibodies to LGALS3BP: A novel biomarker for cancer. Dis Markers 35: 747-752, 2013.
33. Fukawa T, Ono M, Matsuo T, Uehara H, Miki T, Nakamura Y, Kanayama HO and Katagiri T: DDX31 regulates the p53-HDM2 pathway and rRNA gene transcription through its interaction with NPM1 in renal cell carcinoma. Cancer Res 72: 5867-5877, 2012.
34. Hang HC, Yu C, Ten Hagen KG, Tian E, Winans KA, Tabak LA and Bertozzi CR: Small molecule inhibitors of mucin-type O-linked glycosylation from a uridine-based library. Chem Biol 11: 337-345, 2004.
35. Ono M, Shitashige M, Honda K, Isobe T, Kuwabara H, Matsuzuki H, Hirohashi S and Yamada T: Label-free quantitative proteomics using large peptide data sets generated by nanoflow liquid chromatography and mass spectrometry. Mol Cell Proteomics 5: 1338-1347, 2006.
36. Hohenester E, Sasaki T and Timpl R: Crystal structure of a scavenger receptor cysteine-rich domain sheds light on an ancient superfamily. Nat Struct Biol 6: 228-232, 1999.
37. Hellstern S, Sasaki T, Fauser C, Lustig A, Timpl R and Engel J: Functional studies on recombinant domains of Mac-2-binding protein. J Biol Chem 277: 15690-15696, 2002.
38. Sasaki T, Brakebusch C, Engel J and Timpl R: Mac-2 binding protein is a cell-adhesive protein of the extracellular matrix which self-assembles into ring-like structures and binds beta1 integrins, collagens and fibronectin. EMBO J 17: 1606-1613, 1998.
39. Müller SA, Sasaki T, Bork P, Wolpensinger B, Schulthess T, Timpl R, Engel A and Engel J: Domain organization of Mac-2 binding protein and its oligomerization to linear and ring-like structures. J Mol Biol 291: 801-813, 1999.
40. Stampolidis P, Ullrich A and Iacobelli S: LGALS3BP, lectin galactoside-binding soluble 3 binding protein, promotes oncogenic cellular events impeded by antibody intervention. Oncogene 34: 39-52, 2015.
41. Fogeron ML, Müller H, Schade S, Dreher F, Lehmann V, Kühnel A, Scholz AK, Kashofer K, Zerck A, Fauler B, *et al*: LGALS3BP regulates centriole biogenesis and centrosome hypertrophy in cancer cells. Nat Commun 4: 1531, 2013.
42. Cancer Genome Atlas Network: Comprehensive molecular portraits of human breast tumours. Nature 490: 61-70, 2012.
43. Ciriello G, Gatza ML, Beck AH, Wilkerson MD, Rhie SK, Pastore A, Zhang H, McLellan M, Yau C, Kandoth C, *et al*: Comprehensive molecular portraits of invasive lobular breast cancer. Cell 163: 506-519, 2015.
44. Györffy B, Lanczky A, Eklund AC, Denkert C, Budczies J, Li Q and Szallasi Z: An online survival analysis tool to rapidly assess the effect of 22,277 genes on breast cancer prognosis using microarray data of 1,809 patients. Breast Cancer Res Treat 123: 725-731, 2010.